

PREPARATION OF Mg-DOPED TiO₂ NANOPARTICLES FOR PHOTOCATALYTIC DEGRADATION OF SOME ORGANIC POLLUTANTS

MASOUD GIAHI^{a*}, DEEPAK PATHANIA^b, SHILPI AGARWAL^c,
GOMAA A. M. ALI^{d,e}, KWOK FENG CHONG^e,
VINOD KUMAR GUPTA^{c*}

ABSTRACT. In this study, the sol-gel method was used to prepare Mg-doped TiO₂ nanoparticles from titanium tetraisopropoxide and magnesium sulfate as the dopant precursors. Mg-doped TiO₂ shows the formation of anatase phase with polyhedral and spherical particles with an average size of 25-30 nm. X-ray diffraction, X-ray photoelectron spectroscopy, transmission electron microscopy and photoluminescence were used to characterize the prepared material. The photocatalytic degradation performance of rhodamine B, nonylphenol ethoxylates, pseudoephedrine hydrochloride, and nicotine on Mg-doped TiO₂ was studied under UV irradiation. The photocatalytic degradation shows that 98.92, 98.00, 98.00 and 97.95% of rhodamine B, nonylphenol ethoxylates, pseudoephedrine hydrochloride, and nicotine was decomposed by Mg-doped TiO₂, respectively.

Keywords: Mg-doped TiO₂; Organic pollutants; Photocatalytic degradation; Photoluminescence; Sol-gel

^a Islamic Azad University, Department of Chemistry, South Tehran Branch, Tehran, Iran

^b Central University of Jammu, Department of Environmental Sciences, Samba, Jammu and Kashmir-181143, India

^c Center of Excellence for Advanced Materials Research, Faculty of Science, King Abdulaziz University, Jeddah 21589, Saudi Arabia

^d Al-Azhar University, Faculty of Science, Chemistry Department, Assiut, 71524, Egypt

^e Universiti Malaysia Pahang, Faculty of Industrial Sciences & Technology, Gambang, 26300 Kuantan, Malaysia

* Corresponding authors: m_giahi@azad.ac.ir and vinodfcy@gmail.com

INTRODUCTION

Nowadays, heterogeneous photocatalytic degradation using TiO₂ becomes potentially cost-effective and environmentally sustainable treatment technique [1-3]. TiO₂ is a promising candidate photocatalyst due to its high photocatalytic activity, good chemical and biological stability, high energy efficiency, relatively low-cost and nontoxicity [4]. Due to its photoactivity and photocatalytic ability to degrade contaminants, nanocrystalline TiO₂ is attractive and widely used as a photocatalyst [5-8].

TiO₂ powders in the presence of UV or visible light is used to decompose many organic materials in aqueous solutions [9-11]. Water pollutions in the forms of organic and inorganic substances become a critical environmental problem, where, clean water is one of the strategic issues for human life. Water could be contaminated *via* natural or artificial foreign materials from various sources such as industrial effluents, agricultural runoff and chemical spills [12-19]. These effluents include nonbiodegradable, toxic organic materials [20-22]. Recent studies indicate that during manufacturing and processing operations, a substantial amount toxic organic materials enter into the environment [23, 24].

In this work, we synthesized Mg-doped TiO₂ nanophotocatalyst by sol-gel method and then we applied it for photochemical degradation of some environmental pollutants in aqueous solution in the presence of UV light. The results showed this nanophotocatalyst has a good degradation efficiency for the studied environmental pollutants.

RESULTS AND DISCUSSION

X-ray diffraction

The diffractograms of pure and Mg-doped TiO₂ nanoparticles (0.75 and 1.5 at.%) are shown in Figure 1. It is obvious from the patterns, the anatase phase is the main phase in all samples [25]. However, a weak diffraction peak along (1 1 0) indicating the rutile phase is observed for pure titania showing the formation of a mixed phase structure for this sample. Mg atoms are easily inserted into the crystal lattice of TiO₂ due to small the ionic radius of Mg²⁺ (0.57 Å) compared to than Ti⁴⁺ (0.68 Å) ion [26]. Pure phase was observed with no individual peaks of Mg in the pattern. Moreover, Scherrer's formula was used to calculate the particles size (PS) of Mg-doped TiO₂ [27-29]:

$$PS = \frac{0.89\lambda}{\beta \cos\theta} \quad (1)$$

where λ is the wavelength of the used Cu-K_α radiation ($\lambda = 1.54056 \text{ \AA}$), β is the full width at half maximum *and* θ the scattering angle.

PREPARATION OF Mg-DOPED TiO₂ NANOPARTICLES FOR PHOTOCATALYTIC DEGRADATION OF SOME ORGANIC POLLUTANTS

The calculated grain sizes of pure, 0.75 and 1.5 at.% Mg-doped TiO₂ nanoparticles are 24, 22 and 21 nm, respectively. This proves that the crystallite size was decreased with increasing in Mg doping content. The decrement of crystallite size with Mg can be assigned to the smaller ionic radius of Mg compared to Ti.

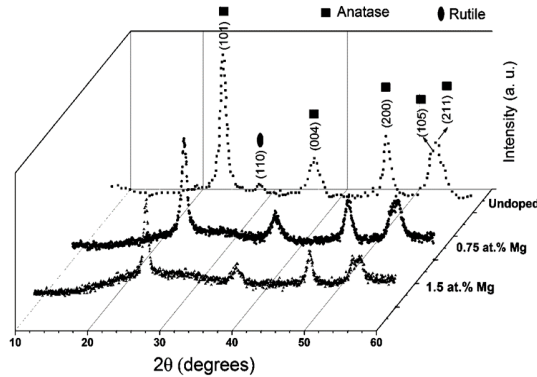


Figure 1. X-ray patterns of pure and Mg-doped TiO₂ nanoparticles.

Transmission electron microscopy analysis

Figure 2 shows the TEM images of the prepared nanoparticles for morphological study. Polyhedral and spherical particles with a particles size of the range 25-30 nm are clearly observed. The particles size obtained from TEM data is in a good agreement with that obtained by XRD calculations. The size of pure TiO₂ is bigger than Mg-doped TiO₂ in both methods. This average grain size is related to different growth orientations [30].

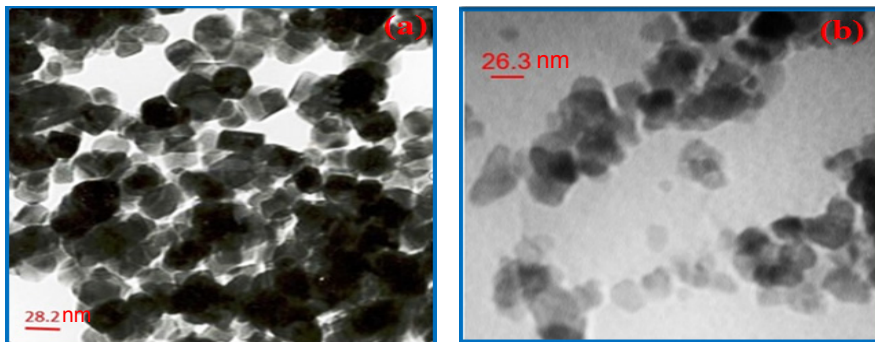


Figure 2. Typical TEM micrographs for undoped (a) and 1.5 at.% Mg-doped TiO₂ (b) nanoparticles.

X-ray photoelectron spectroscopy

To investigate the chemical composition of Mg-doped TiO₂, XPS analysis was performed and displayed in Figure 3. The peaks with binding energies at 458.63 eV and 464.01 eV are ascribed to Ti 2p_{3/2} and Ti 2p_{1/2}. These values are in good agreement with those reported for TiO₂ [31]. The peak at 51.23 eV is related to Mg 2p, which is typical of Mg²⁺ that bonds with an oxygen atom. The inset of Figure 3 gives the atomic percentage of the elements involved in the compound. The presence of a high amount of carbon is expected for the synthesis methods performed in ambient air.

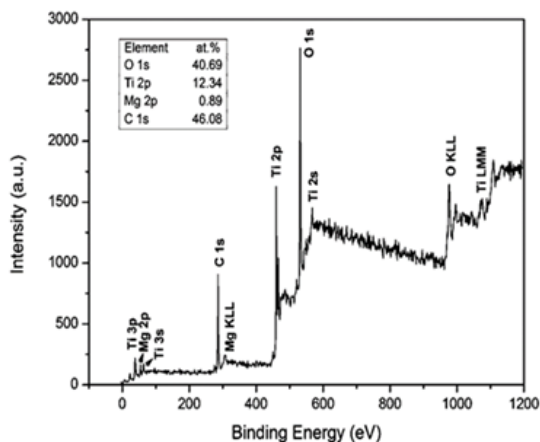


Figure 3. XPS survey spectrum for 1.5 at.% Mg-doped TiO₂ nanoparticles, the inset shows the atomic ratio of the elements.

Photoluminescence spectra

The charge carrier trapping, mobility and transfer to the surface of photocatalysts could be studied using PL spectra. PL spectrum of TiO₂ anatase phase shows broadband as it is an indirect bandgap semiconductor related to radiative recombination of charge carriers. The related PL spectra of the prepared nanoparticles are displayed in Figure 4. The spectra were obtained with an excitation wavelength of 310 nm. The valence band (VB) electrons receive sufficient energy to transfer to the conduction band (CB) when it is irradiated with light of a longer or equal wavelength to its bandgap. These electrons then go back from CB to VB with emission of energy as PL radiation [32]. As it is evident from Figure 4, a strong peak occurs around 356 nm that can be ascribed to the mentioned band-to-band transition. Other PL processes that can take place, include the transfer of excited electrons from CB to other

intermediate bands, *via* non-radiative process, and from the intermediate bands to VB by radiative transition causing PL signals [33]. The inset of Figure 4 depicts the deconvoluted spectrum for pure TiO₂ nanoparticles. The recombination of electrons-holes in surface defects/surface oxygen vacancies could be seen as a small emission below 356 nm occurs at 341 nm [34]. Meanwhile, the shoulder peak at 370 nm can be attributed to an emission of intermediate band transition of titania. Besides, it is obvious that the peak intensity becomes stronger with the increase of the doping amount of Mg, pointing that a higher amount of Mg brings a higher recombination rate, which may result in an excessive formation of Mg doping from the recombination centre.

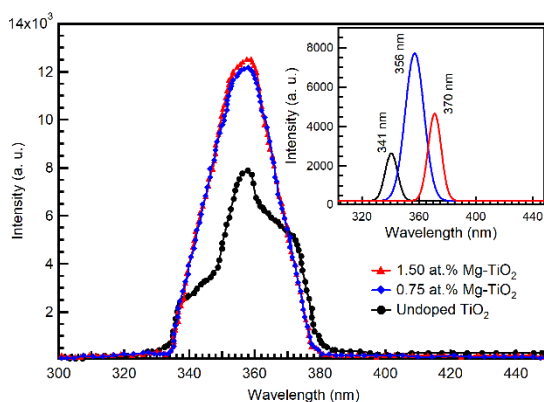


Figure 4. Photoluminescence spectra for pure and 1.5 at.% Mg-doped TiO₂ nanoparticles.

Degradation optimum conditions

To obtain the degradation optimum conditions of rhodamine B, nonylphenol ethoxylates, pseudoephedrine hydrochloride and nicotine, their reactions in the presence of pure TiO₂ and Mg-doped TiO₂ were studied. The photocatalytic degradation (D) was calculated as follows [35]:

$$D(\%) = \frac{(A_0 - A_t)}{A_0} \times 100 \quad (2)$$

where A_0 is the initial absorbance of environmental pollutants and A_t is the absorbance of environmental pollutants after t minutes.

Employing different concentrations of Mg-doped TiO₂ varying from 0.04 to 0.44 g L⁻¹, the effect of initial concentration of the pollutants varying from 10 to 50 mg L⁻¹ and the initial concentration of oxidant such as potassium peroxodisulfate and hydrogen peroxide varying from 1 to 7 mM in pH range of 2.0- 12.0 in the presence of UV light [36-40].

The results, are presented in Figure 5 (rhodamine B), Figure 6 (nonylphenol ethoxylates), Figure 7 (pseudoephedrine hydrochloride) and Figure 8 (nicotine), which indicate that photodegradation efficiency unequivocally increases with increasing irradiation time. In addition, Mg-doped TiO_2 shows high degradation ratios than pure TiO_2 for all organic materials under study. Where the degradation ratio was found to be 98.92, 98.00, 98.00 and 97.95% for rhodamine B, nonylphenol ethoxylates, pseudoephedrine hydrochloride, and nicotine, respectively, in the case of Mg-doped TiO_2 . While, for pure TiO_2 , it was found to be 90.22, 95.00, 91.00 and 91.01% for rhodamine B, nonylphenol ethoxylates, pseudoephedrine hydrochloride, and nicotine, respectively. The optimum conditions for degradation are presented in Figure 9 and listed in Table 1.

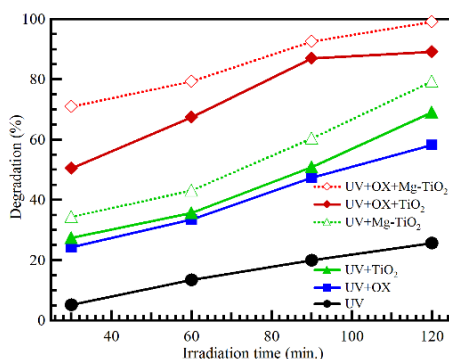


Figure 5. Degradation of rhodamine B in aqueous solutions: conditions are, rhodamine B concentration = 10 mg L^{-1} , pure $\text{TiO}_2 = 0.28 \text{ g L}^{-1}$, Mg-doped $\text{TiO}_2 = 0.20 \text{ g L}^{-1}$, OX ($\text{K}_2\text{S}_2\text{O}_8$) = 3 mM , $\text{pH} = 10$, $V = 25 \text{ mL}$.

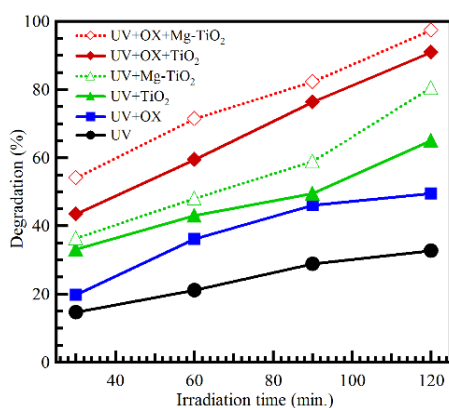


Figure 6. Degradation of nonylphenol ethoxylates in aqueous solutions: conditions are: nonylphenol ethoxylates 6 mol concentration = 20 mg L^{-1} , pure $\text{TiO}_2 = 0.28 \text{ g L}^{-1}$, Mg-doped $\text{TiO}_2 = 0.28 \text{ g L}^{-1}$, OX (H_2O_2) = 1 mM , $\text{pH} = 6$, $V = 25 \text{ mL}$.

PREPARATION OF Mg-DOPED TiO₂ NANOPARTICLES FOR PHOTOCATALYTIC DEGRADATION OF SOME ORGANIC POLLUTANTS

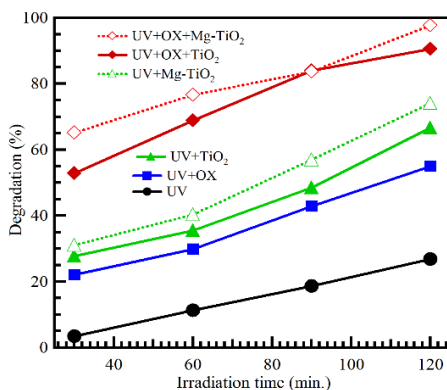


Figure 7. Degradation of pseudoephedrine hydrochloride in aqueous solutions: conditions are, pseudoephedrine hydrochloride concentration = 10 mg L⁻¹, pure TiO₂ = 0.28 g L⁻¹, Mg-doped TiO₂ = 0.28 g L⁻¹, OX (H₂O₂) = 5 mM, pH = 6, V = 25 mL.

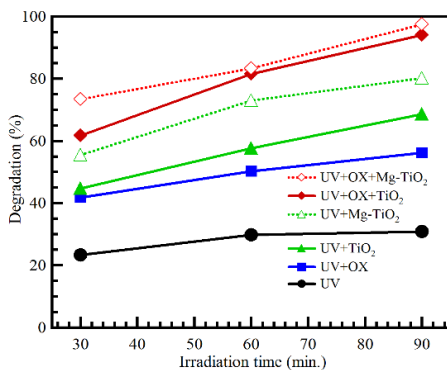


Figure 8. Degradation of nicotine in aqueous solutions: conditions are, nicotine concentration = 20 mg L⁻¹, pure TiO₂ = 0.28 g L⁻¹, Mg-doped TiO₂ = 0.20 g L⁻¹, OX (K₂S₂O₈) = 3 mM, pH = 7, V = 25 mL.

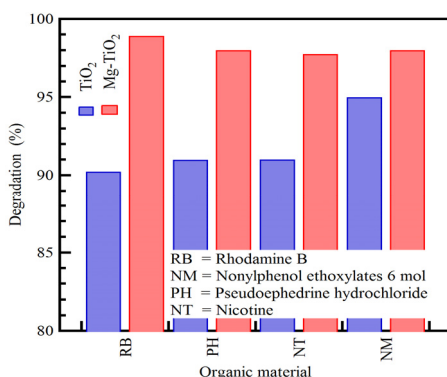


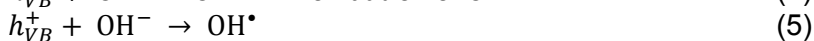
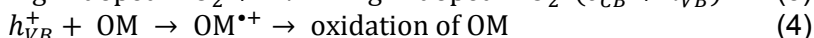
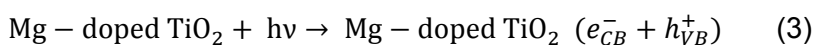
Figure 9. The degradation optimum conditions of the organic pollutants using pure TiO₂ and Mg-doped TiO₂.

Table 1. The degradation optimum conditions of some environmental pollutants using pure TiO₂ and Mg-doped TiO₂.

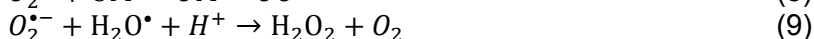
Photocatalyst	Pollutant	Optimum conditions					Degradation (%)
		Conc. of photocatalyst (ppm)	Conc. of pollutant (ppm)	Oxidant (mM)	Irradiation time (min)	pH	
Pure TiO ₂	Rhodamine B	280	10	3 (K ₂ S ₂ O ₈)	90	10	90.22
Mg-doped TiO ₂		200	10	3 (K ₂ S ₂ O ₈)	60	10	98.92
Pure TiO ₂	Nonylphenol ethoxylates	280	20	1 (H ₂ O ₂)	90	6	95.00
Mg-doped TiO ₂		280	20	1 (H ₂ O ₂)	90	6	98.00
Pure TiO ₂	Pseudoephedrine hydrochloride	280	10	5 (H ₂ O ₂)	120	6	91.00
Mg-doped TiO ₂		280	10	5 (H ₂ O ₂)	120	6	98.00
Pure TiO ₂	Nicotine	280	20	3 (K ₂ S ₂ O ₈)	90	7	91.01
Mg-doped TiO ₂		200	20	1 (K ₂ S ₂ O ₈)	90	7	97.95

Degradation mechanism

The photocatalytic degradation of organic material pollutants takes place *via* photoexcitation of the semiconductor and then the formation of an electron-hole pair on the surface of photocatalyst (Eq. 3). The direct oxidation of organic material (OM) to reactive intermediates (Eq. 4) is due to the high oxidative potential of the holes (h_{VB}^+) in photocatalyst. Hydroxyl radicals (OH[•]) are formed either by the reaction of the hole with OH⁻ (Eq. 5) or by water decomposition (Eq. 6). These strong radicals are non-selective oxidants which lead to partial or complete mineralization of several OM [41-46].



Molecular oxygen could be reduced to superoxide anion (Eq. 7) by the action of the conduction band electron (e_{CB}^-) on the catalyst surface. In the presence of organic materials, this radical forms organic peroxides (Eq. 8) or hydrogen peroxide (Eq. 9) [47].



The construction of hydroxyl radicals is due to the conduction band electrons. These radicals have been showed as the primary cause of organic material mineralization [48-50] (Eq. 10).



CONCLUSIONS

In this work, Mg-doped TiO₂ nanoparticles was prepared by the sol-gel method. This photocatalyst was examined by XRD, TEM, XPS and PL analyses. Mg-doped TiO₂ shows polyhedral and spherical particles with an average size of 25-30 nm. The photocatalyst was applied for the degradation of rhodamine B, nonylphenol ethoxylates, pseudoephedrine hydrochloride and nicotine as pollutants. Mg-doped TiO₂ shows a superb degradation of these pollutants between 98-99%.

EXPERIMENTAL PROCEDURE

Materials

Titanium tetraisopropoxide, magnesium sulfate, ethanol, nitric acid, hydrochloric acid, nonylphenol ethoxylates, rhodamine B and nicotine were obtained from Merck. The pseudoephedrine hydrochloride was laboratory prepared and purified.

Preparation of pure and Mg-doped TiO₂ nanoparticles

Initially, solutions A and B were prepared as follows: Solution A, 13.3 mL of absolute ethanol, 2.0 mL of deionized water and magnesium sulfate (0.75 and 1.50 wt.%) were mixed. Solution B, 7.0 mL of titanium tetraisopropoxide and 13.3 mL of absolute ethanol were mixed under stirring for 5 min. Then 1 mL of HNO₃ was added to the prepared mixture drowsily under stirring for 10 min. Then solution A was slowly added to solution B with vigorous stirring until the transparent sol was obtained. The gel was prepared by aging the solution for 48 h at room temperature. The derived gel was dried at 100 °C and then calcined at 400 °C for 4 h. The doping concentrations are expressed as a weight percentage of titanium atoms. Pure TiO₂ is also prepared with the same procedure without adding magnesium sulfate.

Characterizations

The crystalline structure and phase purity were investigated using X-ray diffraction (XRD) by a BRUKER D8 ADVANCE X-ray diffractometer. The morphologies and elemental analyses were determined by transmission electron microscopy (TEM) and X-ray photoelectron spectroscopy (XPS), respectively. The charge carrier trapping, mobility and transfer to the surface of the photocatalysts were studied using photoluminescence (PL) spectroscopy.

Photocatalytic reactor and degradation procedure

Photodegradation experiments were performed with a thermostatic cylindrical Pyrex reactor with a 50 mL capacity reactor system under the irradiation of a UV lamp. A mercury lamp (36 W) was used as UV light source. Around 25 mL of the four environmental pollutant solutions (rhodamine B, nonylphenol ethoxylates, pseudoephedrine hydrochloride and nicotine) with a primary concentration of 20 mg L⁻¹ was placed into the Pyrex reactor. A known amount of Mg-doped TiO₂ photocatalyst (5 and 7 mg, equivalent to 200 and 280 ppm, respectively) was added to the pollutant solution and oxidant (Table 1). Diluted HCl and NaOH solutions were used to adjust the pH. The mixture was then irradiated with the UV lamp up to 120 min. Magnetically stirring (60 rpm) was used throughout the experiment. At regular time intervals, 1 mL was withdrawn then diluted to 5 mL, centrifuged and the absorbance was measured. The quantitative estimation of the environmental pollutants was carried out using a UV-Vis spectrophotometer (Model Jenway 6405) at their λ_{\max} .

ACKNOWLEDGMENT

Financial support by Lahijan Branch, Islamic Azad University Grant No. 17.20.5.3515 is gratefully acknowledged.

REFERENCES

1. W. Baran, E. Adamek, A. Sobczak, A. Makowski, *Applied Catalysis B: Environmental*, **2009**, 90, 516.
2. T.A. Devi, N. Ananthi, T.P. Amaladhas, *Journal of Nanostructure in Chemistry*, **2015**, 6, 75.
3. Y.-X. Zhang, Y. Jia, *Materials Science and Engineering: B*, **2018**, 228, 123.
4. O. Moradi, K. Zare, M. Monajjemi, M. Yari, H. Aghaie, *Fullerenes, Nanotubes and Carbon Nanostructures*, **2010**, 18, 285.
5. A. Abbasi, J.J. Sardroodi, *Journal of Nanostructure in Chemistry*, **2017**, 7, 345.

6. V.R. Posa, V. Annavaram, A.R. Somala, *Bulletin of Materials Science*, **2016**, 39, 759.
7. É. Karácsonyi, L. Baia, A. Dombi, V. Danciu, K. Mogyorósi, L. Pop, G. Kovács, V. Coşoveanu, A. Vulpoi, S. Simon, *Catalysis today*, **2013**, 208, 19.
8. Z. Pap, É. Karácsonyi, L. Baia, L.C. Pop, V. Danciu, K. Hernádi, K. Mogyorósi, A. Dombi, *Physica Status Solidi (b)*, **2012**, 249, 2592.
9. F. Abbaszadeh, O. Moradi, M. Norouzi, O. Sabzevari, *Journal of Industrial and Engineering Chemistry*, **2014**, 20, 2895.
10. N.S. Begum, H.M. Farveez Ahmed, *Bulletin of Materials Science*, **2008**, 31, 43.
11. G. Zhao, J. Zou, C. Li, J. Yu, X. Jiang, Y. Zheng, W. Hu, F. Jiao, *Journal of Materials Science: Materials in Electronics*, **2018**, 29, 7002.
12. M.S. Derakhshan, O. Moradi, *Journal of Industrial and Engineering Chemistry*, **2014**, 20, 3186.
13. S.M.S. Arabi, R.S. Lalehloo, M.R.T.B. Olyai, G.A.M. Ali, H. Sadegh, *Physica E: Low-dimensional Systems and Nanostructures*, **2019**, 106, 150.
14. H. Sadegh, G.A.M. Ali, A.S.H. Makhlof, K.F. Chong, N.S. Alharbi, S. Agarwal, V.K. Gupta, *Journal of Molecular Liquids*, **2018**, 258, 345.
15. S.P. Lee, G.A.M. Ali, H. Algarni, K.F. Chong, *Journal of Molecular Liquids*, **2018**, 277, 175.
16. H. Sadegh, G.A.M. Ali, V.K. Gupta, A.S.H. Makhlof, R. Shahryari-ghoshekandi, M.N. Nadagouda, M. Sillanpää, E. Megiel, *Journal of Nanostructure in Chemistry*, **2017**, 7, 1.
17. O.A. Habeeb, K. Ramesh, G.A.M. Ali, R.M. Yunus, *Desalination and Water Treatment*, **2017**, 84, 205.
18. H. Sadegh, G.A.M. Ali, Z. Abbasi, M. N. Nadagouda, *Studia Universitatis Babeş-Bolyai Chemia*, **2017**, 62, 233.
19. S. Agarwal, H. Sadegh, M. Majid, A.S.H. Makhlof, G.A.M. Ali, A.O.H. Memar, R. Shahryari-ghoshekandi, I. Tyagi, V.K. Gupta, *Journal of Molecular Liquids*, **2016**, 218, 191.
20. H.H. Abdel Ghafar, G.A.M. Ali, O.A. Fouad, S.A. Makhlof, *Desalination and Water Treatment*, **2015**, 53, 2980.
21. V.K. Gupta, S. Agarwal, H. Sadegh, G.A.M. Ali, A.K. Bharti, A.S. Hamdy, *Journal of Molecular Liquids*, **2017**, 237, 466.
22. K. Byrappa, A.K. Subramani, S. Ananda, K.M.L. Rai, R. Dinesh, M. Yoshimura, *Bulletin of Materials Science*, **2006**, 29, 433.
23. S. Samadi, M. Yousefi, F. Khalilian, A. Tabatabaee, *Journal of Nanostructure in Chemistry*, **2014**, 5, 7.
24. S. Agarwal, H. Sadegh, M. Monajjemi, A.S. Hamdy, G.A.M. Ali, A.O.H. Memar, R. Shahryari-ghoshekandi, I. Tyagi, V.K. Gupta, *Journal of Molecular Liquids*, **2016**, 218, 191.
25. H.-S. Kil, Y.-J. Jung, J.-I. Moon, J.-H. Song, D.-Y. Lim, S.-B. Cho, *Journal of Nanoscience and Nanotechnology*, **2015**, 15, 6193.
26. H.S. Wahab, A.A. Hussain, *Journal of Nanostructure in Chemistry*, **2016**, 6, 261.
27. A. Patterson, *Physical Review*, **1939**, 56, 978.

28. O.A. Fouad, G.A.M. Ali, M.A.I. El-Erian, S.A. Makhlof, *Nano*, **2012**, 7, 1250038.
29. O.A. Fouad, S.A. Makhlof, G.A.M. Ali, A.Y. El-Sayed, *Materials Chemistry and Physics*, **2011**, 128, 70.
30. N. Rohani, F.F. Bamoharram, A. Marjani, M.M. Heravi, *Journal of Nanostructure in Chemistry*, **2017**, 7, 171.
31. B.S. Surendra, M. Veerabhdraswamy, K.S. Anantharaju, H.P. Nagaswarupa, S.C. Prashantha, *Journal of Nanostructure in Chemistry*, **2018**, 8, 45.
32. M. Mohamed Jaffer Sadiq, A. Samson Nesaraj, *Journal of Nanostructure in Chemistry*, **2014**, 5, 45.
33. O. Moradi, M. Aghaie, K. Zare, M. Monajjemi, H. Aghaie, *Journal of Hazardous Materials*, **2009**, 170, 673.
34. B. Shariatzadeh, O. Moradi, *Polymer Composites*, **2014**, 35, 2050.
35. R. Zeynolabedin, K. Mahanpoor, *Journal of Nanostructure in Chemistry*, **2017**, 7, 67.
36. D. Robati, B. Mirza, R. Ghazisaeidi, M. Rajabi, O. Moradi, I. Tyagi, S. Agarwal, V.K. Gupta, *Journal of Molecular Liquids*, **2016**, 216, 830.
37. S. Agarwal, I. Tyagi, V.K. Gupta, F. Golbaz, A.N. Golikand, O. Moradi, *Journal of Molecular Liquids*, **2016**, 218, 494.
38. M. Noei, M. Ebrahimikia, N. Molaei, M. Ahadi, A.A. Salan, O. Moradi, *Russian Journal of Physical Chemistry A*, **2016**, 90, 2221.
39. B. Enayatpour, M. Rajabi, M. Yari, S.M. Reza Mirkhan, F. Najafi, O. Moradi, A.K. Bharti, S. Agarwal, V.K. Gupta, *Journal of Molecular Liquids*, **2017**, 231, 566.
40. M. Rajabi, K. Mahanpoor, O. Moradi, *RSC Advances*, **2017**, 7, 47083.
41. H. Mahmoodian, O. Moradi, B. Shariatzadeha, T.A. Salehf, I. Tyagi, A. Maity, M. Asif, V.K. Gupta, *Journal of Molecular Liquids*, **2015**, 202, 189.
42. F. Najafi, O. Moradi, M. Rajabi, M. Asif, I. Tyagi, S. Agarwal, V.K. Gupta, *Journal of Molecular Liquids*, **2015**, 208, 106.
43. M. Yari, M. Rajabi, O. Moradi, A. Yari, M. Asif, S. Agarwal, V.K. Gupta, *Journal of Molecular Liquids*, **2015**, 209, 50.
44. M. Giah, N. Badalpoor, S. Habibi, H. Taghavi, *Bulletin of the Korean Chemical Society*, **2013**, 34, 2176.
45. M. Giah, S. Saadat Niavol, H. Taghavi, M. Meskinfam, *Russian Journal of Physical Chemistry A*, **2015**, 89, 2432.
46. L.-C. Pop, I. Tantis, P. Lianos, *International journal of hydrogen energy*, **2015**, 40, 8304.
47. J. Wang, G. Liu, Y. Liu, C. Zhou, Y. Wu, *CLEAN–Soil, Air, Water*, **2017**,
48. D. Robati, B. Mirza, M. Rajabi, O. Moradi, I. Tyagi, S. Agarwal, V.K. Gupta, *Chemical Engineering Journal*, **2016**, 284, 687.
49. M. Rajabi, B. Mirza, K. Mahanpoor, M. Mirjalili, F. Najafi, O. Moradi, H. Sadegh, R. Shahryari-ghoshekandi, M. Asif, I. Tyagi, S. Agarwal, V.K. Gupta, *Journal of Industrial and Engineering Chemistry*, **2016**, 34, 130.
50. D. Robati, M. Rajabi, O. Moradi, F. Najafi, I. Tyagi, S. Agarwal, V.K. Gupta, *Journal of Molecular Liquids*, **2016**, 214, 259.